Design of an Experimentally Simulated Moving Bed Reactor for Oxidative Coupling of Methane

Undergraduate Research Thesis in Chemical Engineering

Presented in Partial Fulfillment of the Requirements for Graduation with Honors Research Distinction from the Department of Chemical and Biomolecular Engineering at The Ohio State University

Written By:

William Drees

April 2017

Honors Thesis Committee:

Dr. Liang-Shih Fan

Dr. David Tomasko

Abstract

With the recent increase in natural gas production, methane has become an increasingly attractive compound with which to upgrade to higher value products such as ethylene. One method of great interest, the oxidative coupling of methane, has been prevented from commercialization by low yield caused mainly by reaction of intermediates and products with gas phase oxygen. This makes a chemical looping reaction scheme very attractive because in this scheme, oxygen is delivered via the lattice oxygen on a catalytic oxygen carrier (COC) eliminating gas phase oxygen contact with any hydrocarbon species. In a chemical looping scheme, a moving bed reducer reactor is typically used in which the reactant methane gas and solid COC can travel in either co-current or counter-current configurations. These two moving bed configurations were experimentally simulated using two fixed-bed reactors with each fixed-bed reactor containing COC with different degrees of oxidation. From these studies, it is predicted that a co-current moving bed reactor would provide better yields than a counter-current moving bed reactor due to the increased selectivity of the reduced COC that would be present near the gas outlet of the reactor in the co-current configuration. This more selective, reduced COC would minimize over-oxidation of hydrocarbon products at the gas outlet that were formed in earlier stages of the reactor.

Acknowledgements

I would like to give my greatest thanks to Dr. Liang-Shih Fan for the opportunity to do undergraduate research in his group, advising me throughout this undergraduate research process and for his valuable feedback and guidance. I would also like to thank Dr. Tomasko for being part of my committee and for his guidance through this process.

I would like to give special thanks to both Deven Baser and Sourabh Nadgouda for their sacrifice of significant amounts of time helping me to collect and analyze data as well as teaching me about laboratory techniques, experimental investigation, chemical looping, and chemical engineering in general. In addition, I would like to thank them for their valuable recommendations to improve the various presentations and written reports (including this thesis) that I was able to take part in during my undergraduate career. I would also like to thank Dr. Elena Chung for her mentorship, guidance, and motivation in the early parts of my undergraduate career. I would also like to thank William Wang, Dr. Andrew Tong, and Dr. Mandar Kathe for guidance during various parts of my undergraduate research. Thank you, also, to the various undergraduate students that I had the pleasure of working with in Dr. Fan's lab for your companionship and aid in experiments.

Finally, I would like to thank my parents, William and Marian Drees. Their stress on morals and values helped to shape me into the person I am today and it was their drive for me to accomplish all of my goals that kept me striving and motivated throughout my life to reach the levels of success that I have.

Table of Contents

List of Figures

List of Tables

1. Introduction

Ethylene is the most produced organic chemical with market demand greater than 150 million tons per year with a projected global growth rate of 3.5% [1]. As a result of this demand, researches have, for decades, investigated alternative methods of ethylene production focusing on low cost feedstocks combined with process intensification for new ethylene synthesis routes. One particular feedstock of interest is methane. Recent developments in hydraulic fracturing drilling technology have significantly increased the production of natural gas, composed mostly of methane, both in the United States and around the world. Figure 1 below displays this increase over the past 10 years and this trend is expected to continue [2].

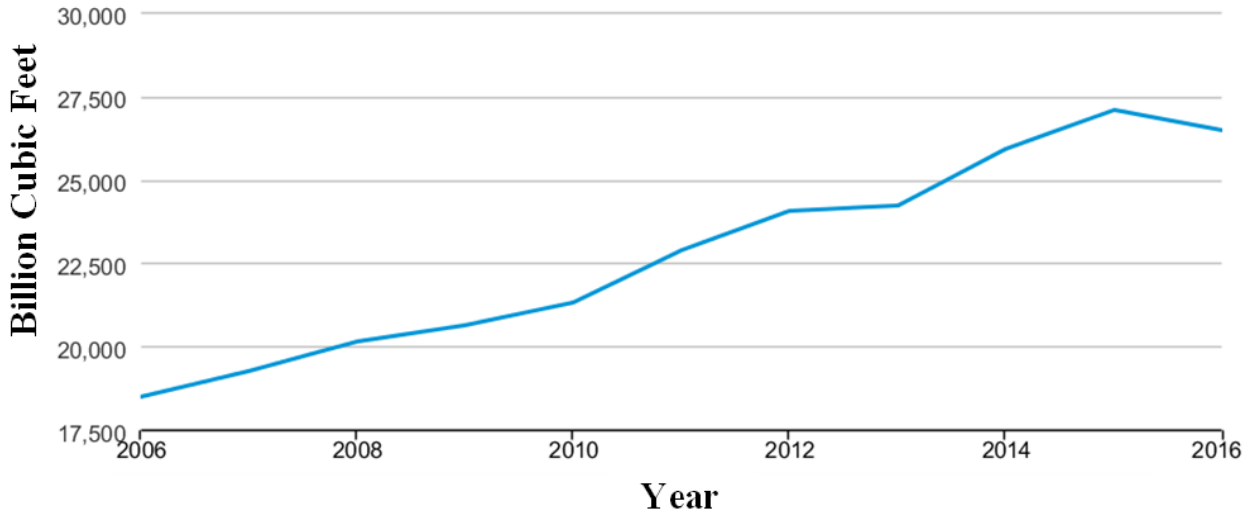

Figure 1: Trend of Natural Gas Production over the past 10 years

As a result of increasing ethylene demand combined with increased natural gas and methane production, researchers have been highly focused on the conversion of methane to ethylene. Several processes are possible which require two or more steps such as methane to methanol to ethylene and methane to syngas to ethylene but a direct conversion of methane to ethylene, known as the oxidative coupling of methane (OCM), is the most economically attractive for commercial realization.

1.1. Oxidative Coupling of Methane Overview

1.1.1. History and Mechanism

The OCM reaction first gained major interest in the 1982 after Keller and Bhasin's large scale experimental screening of metal oxides [3]. Since this time, thousands of complex metal oxide formulations have been investigated both in academic and industrial settings. However, due to lack of success resulting in no commercial realization, interest faded in the early 2000's until the previously mentioned increase in natural gas production revitalized interest in the subject. Shown in Figure 2 below is the trend of published journal articles related to OCM which shows this recent revitalization of interest in OCM [4].

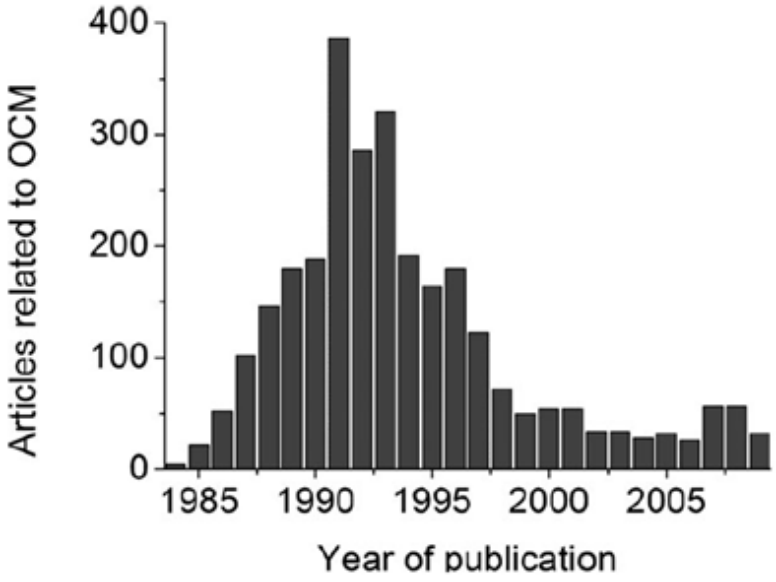

Figure 2: Trend of journal publication related to OCM since the 1980's

A simplified chemical reaction for OCM is shown in Figure 3 below. This figure is simplified because carbon oxides (CO_2 and CO), saturated hydrocarbons, and higher order hydrocarbons can also be produced in this reaction depending on the nature of the catalyst. The oxygen can also be delivered in different ways which will be discussed in section 1.2.

$$2CH_4 + \frac{1}{2}O_2 \rightarrow H_2O + C_2H_6$$

Figure 3: General OCM reaction

The mechanism of this reaction is fairly complex involving both gas-phase and surface reactions. The role of the catalyst is to extract a hydrogen atom from methane forming a methyl radical species at the site of a surface oxygen atom through a Mars-van Krevelen mechanism (the surface hydroxyl group will eventually leave the surface as water leaving an oxygen vacancy for gaseous oxygen to fill and repeat the reaction) [5]. This methyl radical enters the gas phase to couple with another methyl radical forming ethane. The hydrogen atoms of ethane can then be abstracted in a similar manner through a surface oxygen forming ethylene. This process is summarized in Figure 4 below [6].

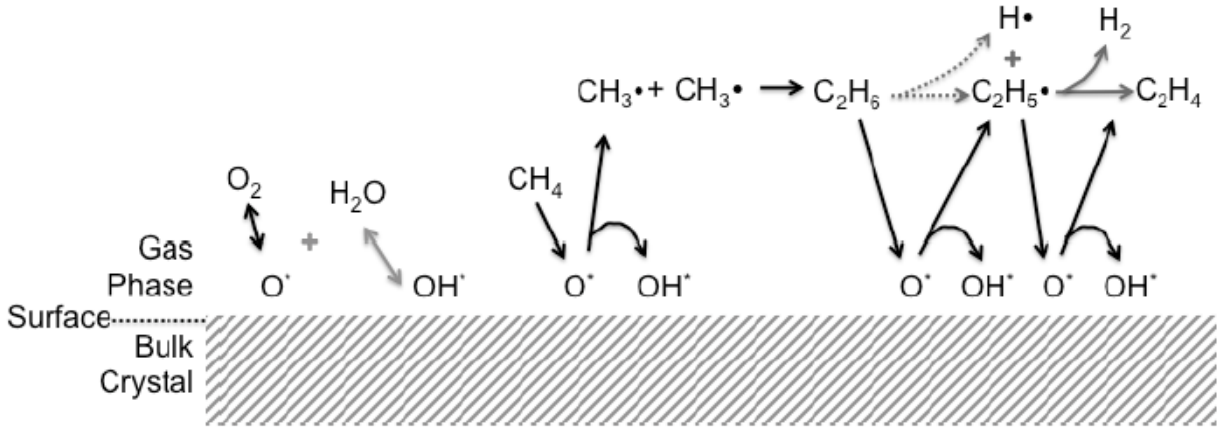

Figure 4: Mechanism of the OCM reaction

1.1.2. Limitations to Commercialization

Despite the research interest in OCM, no commercial scale projects have found success. The current method of ethylene production involves the thermal cracking, known as pyrolysis, of hydrocarbons with steam to form intermediates which can then undergo dehydrogenation. This cracking and dehydrogenation process is endothermic requiring large amounts of heat input

limiting the attractiveness of the pyrolysis process. In addition, as shown in Figure 5 below, the major hydrocarbon source for ethylene production by pyrolysis is naphtha [7]. With the increase in natural gas production, the price differential of methane to naphtha is expected to steadily widen favoring methane as a feedstock helping to make OCM a more economically attractive process.

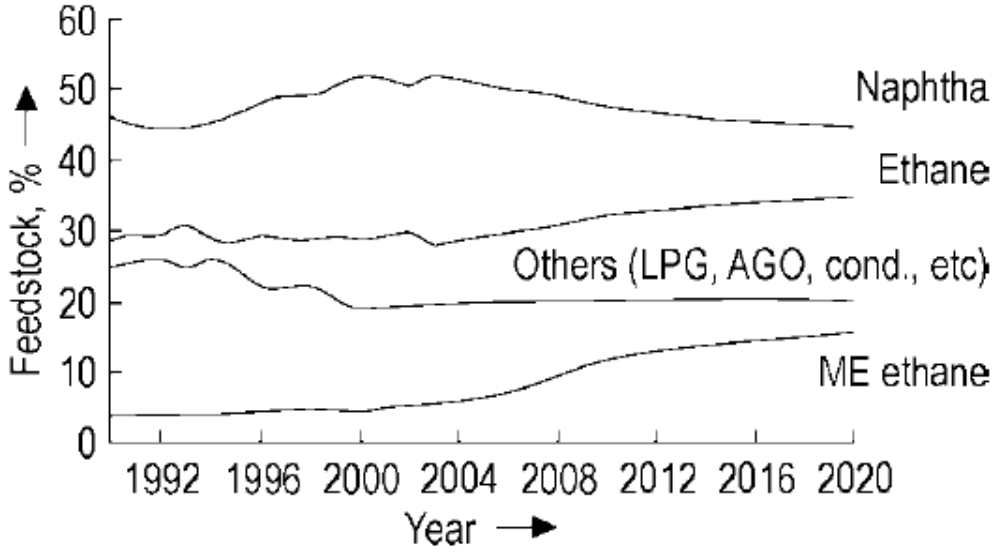

Figure 5: Feedstocks used for ethylene production

The major barrier to OCM commercialization, however, is the limited yield of ethylene. Kinetic and mechanistic studies have identified an upper limit on yields of around 28% per reactor pass for conventional, packed-bed, continuous-feed operations [8, 9]. These yields are well below the estimated target of 35% needed for commercialization [10]. As a result, identification of non-conventional reaction schemes has become the focus of many OCM studies and is the focus of this research.

1.2 Chemical Looping for OCM

A potential method of improving yields in the OCM process is through the application of a chemical looping scheme. In this scheme, the catalyst participates in the reaction by undergoing reduction and oxidation in separate reactors. The catalyst is referred to as a catalytic

oxygen carrier (COC) when it participates in the reaction in this manner. The general scheme is depicted in Figure 6 below [11]. As shown in the figure, the oxidized COC enters the reducer reactor where it reacts with methane and becomes reduced in the OCM reaction described in Figure 3 above. The reduced COC then enters a combustor reactor where it is re-oxidized with air to repeat the process.

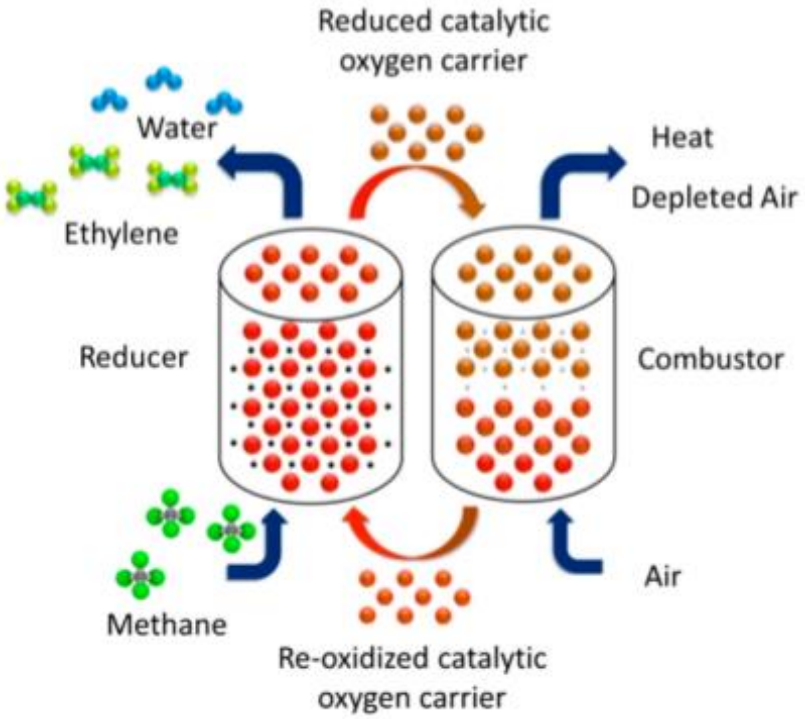

Figure 6: Chemical looping process for OCM

In this process, the COC delivers its lattice oxygen to methane for the OCM reaction and gas phase oxygen is eliminated from the methane reaction which has been found to significantly increase selectivities to ethane, ethylene, and higher hydrocarbon formation by reducing over-oxidation [3, 12]. In this scheme, the COC is transient in nature giving different selectivities and conversions dependent on how far the COC has been reduced requiring lab-scale experiments to be more sophisticated than those for a fixed-bed, co-feed oxygen and methane reactor.

1.3 Experimentally Simulated Moving Bed Reactor

The reducer reactor in the chemical looping scheme can be designed in a number of different ways, each with their own impact on the yield of the OCM reaction. The reactor scheme of most interest is a moving-bed reactor. This reactor was identified as the most attractive because of the short contact times between the reactant gas and solid COC which is required for the OCM reaction as well as limited back-mixing for both the gas and solid phases. Another reason that the moving bed reactor was chosen is that it is already being utilized commercially. One major example is a fluidized catalytic cracking unit which uses a moving bed riser reactor to contact the solid catalyst with the liquid and gas reactants for a very brief time before their separation.

1.3.1 Possible Reducer-Reactor Moving-Bed Configuration

Within the realm of moving bed reactors, there are 3 main configurations to consider: co-current, counter-current, and cross-current. The co-current moving bed reactor scheme is shown in Figure 7(a) below. As shown in the figure, the gas and solid flow in the same direction within the reactor. As a result, when the gas first enters the reactor, it contacts with fresh, oxidized COC where reaction occurs. As the product gases and COC move through the reactor, the COC begins to become more reduced changing the activity of the COC. Figure 7(b) shows a counter-current bed where the reactant gases and COC move in the opposite directions. In this configuration, the gas initially contacts an already reduced COC when it first enters the reactor and as the gas moves through the reactor, it sees a more and more oxidized COC before seeing a fresh, fully oxidized COC at the gas exit of the reactor. Figure 7(c) shows a cross-current moving bed reactor. In this configuration, the reactant gases are initially exposed to the COC at all of its oxidation stages. This reactor scheme was not investigated due to additional complications

involved with development of a gas-permeable membrane reactor but is the topic of other research [13].

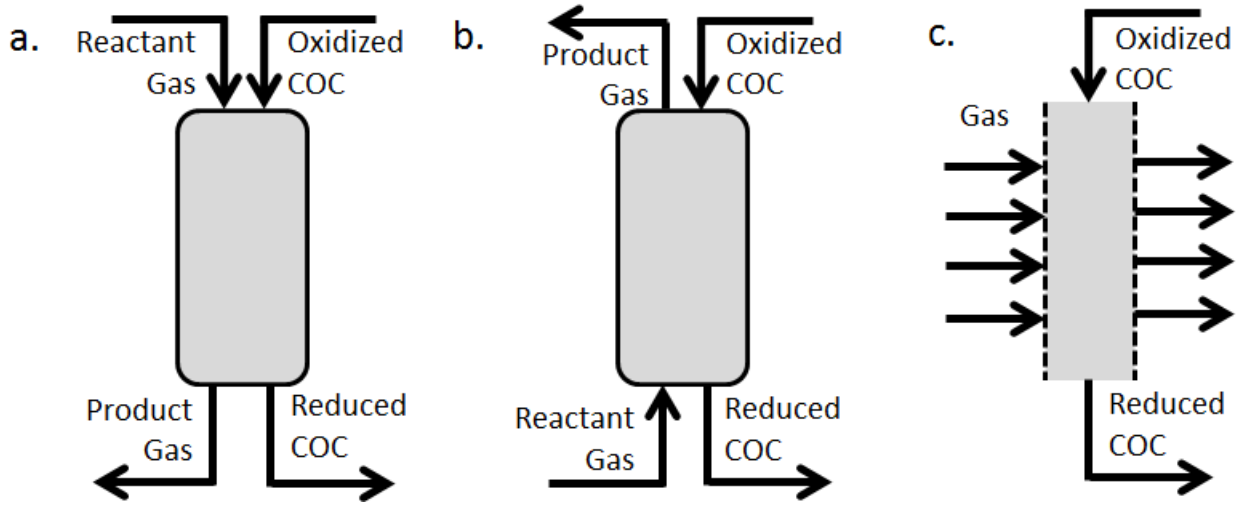

Figure 7: (a) co-current moving bed diagram; (b) counter-current moving bed diagram; (c) cross-current moving bed diagram

When comparing the co-current and counter-current moving bed reactors, the major point of comparison is the profile of the COC's degree of oxidation that the gas encounters as it moves through the bed. For the co-current configuration, as discussed above, the gas initially contacts fresh, fully oxidized COC where the concentration of available lattice oxygen, denoted [O], is at a maximum. As the gases move through the reactor with the COC, the lattice oxygen in the COC decreases until it reaches a minimum at the exit of the reactor. An estimation of the lattice oxygen profile is shown below in Figure 8(a) assuming the gas and solid COC enter the reactor at position 0 and leave at position L. For the counter-current configuration, the gas initially contacts a COC that has lost much of its available lattice oxygen and this lattice oxygen is at a minimum. As the gas moves through the reactor, the COC that it makes contact with contains more and more lattice oxygen until at the gas exit of the reactor where the lattice oxygen on the COC is at a maximum. This is shown below in Figure 8(b) assuming that the gas enters the reactor at position 0 and leaves at position L while the solid COC enters at position L and exits at

position 0. These profiles shown in Figure 8 are only estimates as the true profile was not mapped out as a part of this investigation.

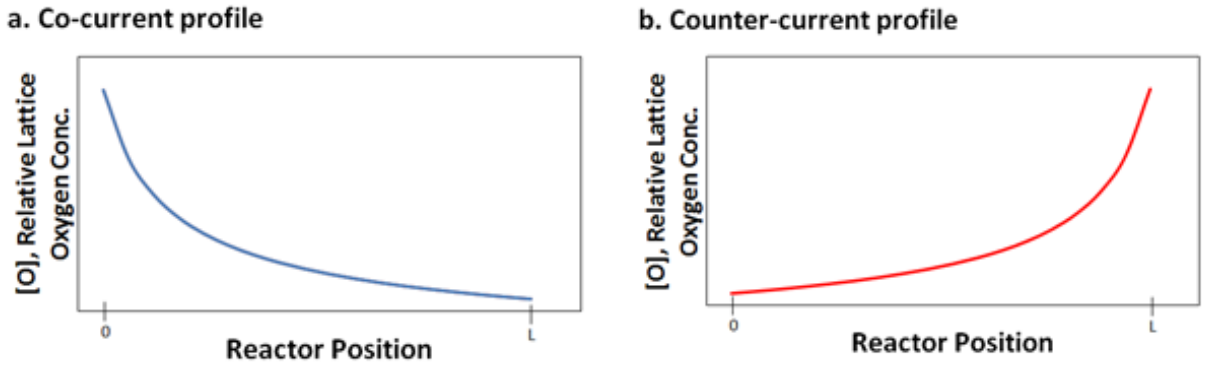

Figure 8: Approximate available lattice oxygen profile for (a) co-current moving bed configuration and (b) counter-current moving bed configuration

1.3.2 Limitations of a Single Fixed Bed Reactor

Traditionally, the chemical looping scheme for OCM has been studied by modulating the flow of reducing and oxidizing gases, methane and air respectively, over the COC in a fixed bed. In fact, in the pioneering OCM work by Keller and Bhasin, a fixed bed reactor used alternating flow of CH_4, which reduces the COC and forms products, followed by air, to oxidize and regenerate the catalyst in repeating cycles [3]. Although this reactor set-up is simple for lab scale catalyst screening, it cannot capture the effects of different moving bed reactor designs. In this traditional, redox fixed bed, when methane is introduced, the front portion of the bed begins to reduce as its lattice oxygen is consumed at a high rate in the conversion of methane. This is a result of the fast reduction time for most OCM COC's. This reduced COC then has different reactivity characteristics which usually favor selective reactions at reduced conversion while the later portion of the bed is still fully oxidized giving relatively high conversion at low selectivity. This is shown schematically in Figure 9 below. Comparing Figure 9 with Figure 8 above, the

redox fixed bed experiment's lattice oxygen profile has a similar entrance and exit lattice oxygen profile to the counter-current configuration (where lattice oxygen is at a minimum at the gas entrance and maximum at the gas exit) but fails to capture features of the co-current moving bed configuration.

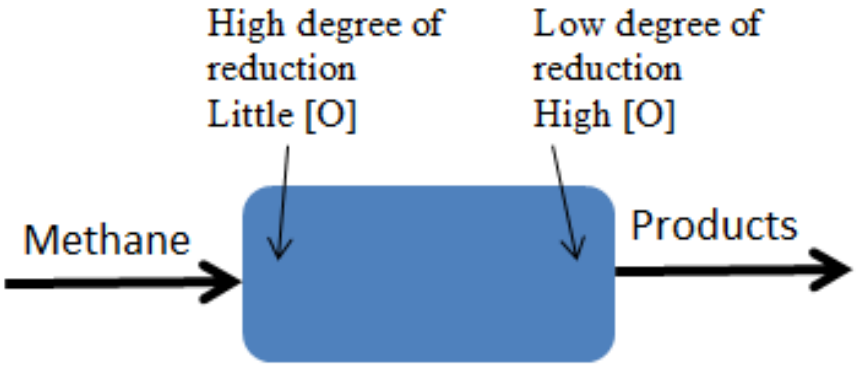

Figure 9: Lattice oxygen characteristics of a modulated fixed bed traditionally used in lab-scale experiments

1.3.3 Moving Bed Evaluation

A simplistic way of evaluating a moving bed reactor is to consider the bed in two portions: one portion of fresh, oxidized COC and the other containing much more reduced COC. Depending on the configuration of the moving bed (co-current or counter-current), the incoming gas will flow through the two different oxidation states in different orders in the reaction flow potentially having a large impact on yield. For example, as shown in Figure 10(a) below, in the co-current configuration, the reactant gases will first pass over the fully oxidized COC then the more reduced COC before leaving the reactor while in the counter-current configuration, Figure 10(b), the flow pattern is the opposite. Since the degree of oxidation of the COC can have a big impact on the reactivity characteristics, this can have a large impact on the overall yield of the COC. This two-bed approach is, of course, a simplified representation. A moving bed reactor

could theoretically be simulated using an infinite number of fixed beds, each with slightly different degrees of oxidation. This two-bed simplistic view of a moving bed reactor, however, will be the groundwork of this thesis and has been studied before generating results that were similar to a true moving bed reactor [14].

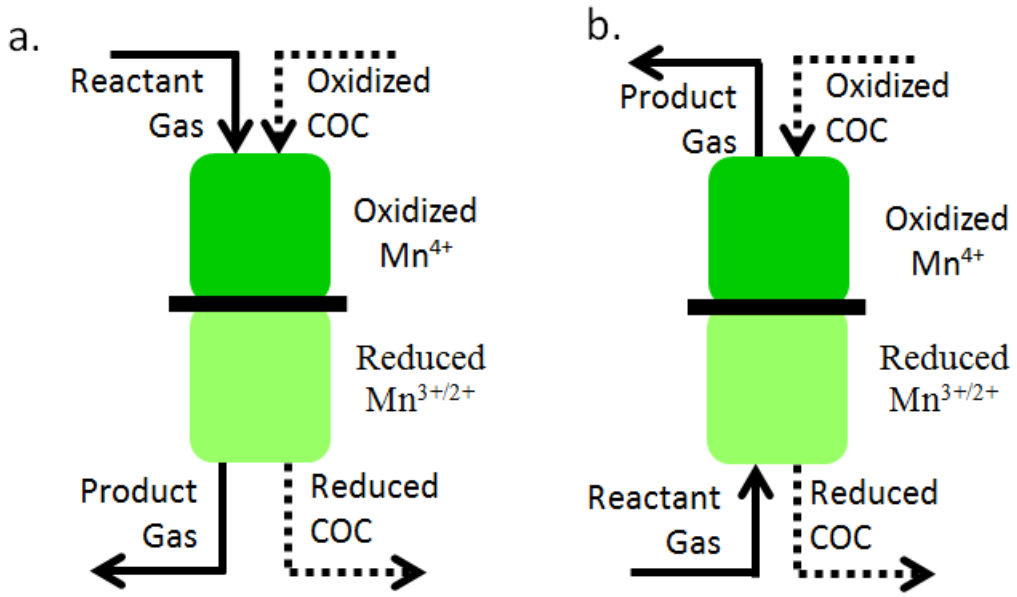

Figure 10: Simplified two-bed flow pattern comparison of gas through (a) co-current moving bed and (b) counter-current moving bed

2. Experimental Methodology

2.1 Catalyst Synthesis

The COC used in all of the following studies is a lithium-doped magnesium-manganese oxide compound. The COC was produced by wet mixing LiOH, MgO, and MnO_2 in stoichiometric ratio to produce $Li_{0.2}Mg_{5.8}MnO_8$. The mixture was then dried before calcination at 950°C in air. COC particles of 300-850 µm were sieved for use. This ternary metal oxide system has been previously studied in literature and has shown to be selective for the OCM reaction [15, 16, 17].

The synthesized COC needed to undergo activation through cycles of oxidation in air for 30 minutes and reduction in methane for 15 seconds which were repeated 10 times. During these activation cycles, changes in selectivity and conversion occurred that prompted further testing to gain a better understanding for the changes that occur during activation. As a result Brunauer–Emmett–Teller (BET) surface area analysis was performed on the fresh and activated samples using pure N_2 as the adsorption/desorption gas in a Quantachrome Nova 4200. For the BET analysis, the samples were first degassed at 300°C for at least 8 hours before multipoint BET analysis was used to determine the surface area of the COC. In addition to the BET surface area analysis, TGA studies, which will be detailed in section 2.2, were performed during the activation of a fresh catalyst as well to identify changes in weight and its behavior over the activation period.

After the COC was activated, a portion was separated and reduced under pure N_2 for 16 hours. This portion was to be used as the reduced COC and will be referred to as the N_2 reduced COC. The fully oxidized COC will be referred to as the oxidized COC.

2.2 Thermogravimetric Analyzer Setup

To understand more about both the oxidized and N_2 reduced COC's, thermogravimetric analyzer (TGA) studies were performed. The instrument used was model SDT Q600 by TA Instruments. The instrument accurately measures changes in weight of the COC under reaction conditions and under the flow of various gases. The first TGA studies focused on the weight difference for the oxidized and N_2 reduced COC. This was done by loading the TGA with oxidized COC and heating to a reaction temperature of 850°C under the flow of 4% O_2/96% N_2 which corresponds to 20% air in 80% N_2 due to limitations of the TGA. Once at temperature, the weight of this oxidized COC was used as the reference of 100% weight. Pure N_2 gas was then flowed in for an extended period of time to remove uncoupling lattice oxygen. Once a steady state had been achieved, 20% CH_4 was flowed in to achieve full reduction of the COC. The relative weights of the oxidized COC, N_2 reduced COC and fully reduced COC were then compared.

The second TGA analysis focused on the relative rate of reduction between the oxidized and N_2 reduced COC, measured as a change in weight, under the flow of 20% CH_4. For analysis of the oxidized COC, a sample was ramped up to reaction temperature of 850°C in 4% O_2/96% N_2 mixture. The reactor was purged for a brief time to remove gaseous O_2 and then 20% CH_2 in N_2 was then pulsed in to investigate the rate of reduction of the oxidized COC. For analysis of the N_2 reduced COC, the COC was heated up in pure N_2 until steady state was achieved followed by the pulsing of 20% CH_4 in N_2 to identify the rate of reduction.

The results of these TGA studies will be compared with the reactivity results of the oxidized and N_2 reduced COC from a previous investigation [18]. In this previous investigation from the same lab, the oxidized and N_2 reduced COC was loaded into a single fixed bed in two

separate trials and methane was pulsed in and the products were collected and analyzed for the first 5 seconds of reaction. This procedure was similar to the procedure for the experimentally simulated moving bed setup described in section 2.3 below. The results of the TGA studies and trends from the reactivity results will be presented to form a hypothesis about which of the simulated moving bed configurations would be expected to provide the greatest yields.

2.3 Experimentally Simulated Moving Bed Reactor Setup

To accurately represent the conditions of co-current and counter-current moving bed reactors, a dual-bed reactor setup was designed and built and is shown in Figure 11 below. The total COC was split between two 2.5 cm^3 COC beds each placed in a ½" ID inert, ceramic reactor. All gas flowrates occurred at 200 mL/min to give a gas hourly space velocity (GHSV) of 2400 h^{-1}. The auxiliary gas port shown in Figure 11 was used to maintain the COC's oxidation state during heat-up of the reactors. Three way valves were used to isolate and couple the two reactor beds when needed. Inert ceramic particles of 1/8" diameter were placed inside the reactor as support and to limit gas residence time in the reactor minimizing thermal cracking of products. When methane was pulsed in, it first flowed through Bed 1 followed by Bed 2. The products were captured for two consecutive five second intervals (0-5 seconds and 5-10 seconds of reaction) and product analysis was performed in an Agilent 7890B gas chromatograph equipped with a thermal conductivity detector and flame ionization detector along with an Agilent 5977A mass spectrometer for confirmation of identified species.

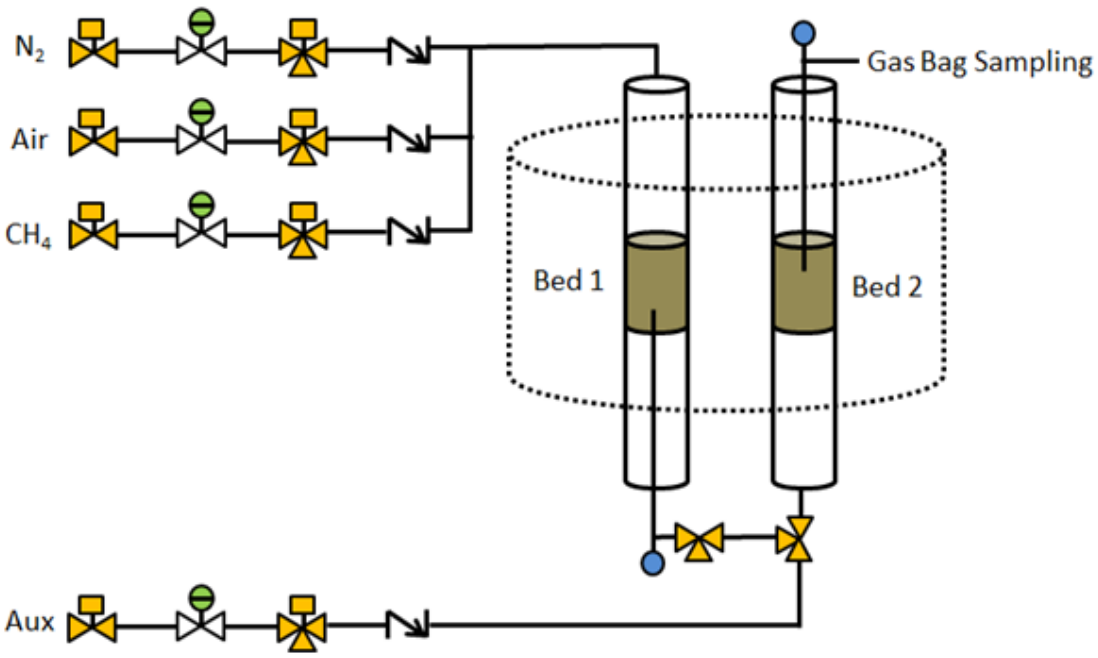

Figure 11: PFD for simulated moving bed reactor setup using 2 fixed beds

The placement of the oxidized and N_2 reduced COC's for each reactor condition is described in Table 1 below and is characteristic the moving bed configuration as shown Figure 10 and discussed in section 1.3.3 above.

Table 1: Locations of the different COC's in the simulated moving bed setup

Bed Configuration	Bed 1	Bed 2
Co-current	Oxidized COC	N_2 Reduced COC
Counter-current	N_2 Reduced COC	Oxidized COC

The values of conversion, selectivity, and yield for the two simulated moving bed configurations will be used for summary and comparison. Their definitions are shown below in Figure 12 where C_i is the mole fraction of compound 'i' and N_{Ci} is the number of carbon atoms in compound 'i'. In the definition of selectivity, the desired products include all hydrocarbon species with at least 2 carbon atoms.

$$\boldsymbol{Selectivity} = \frac{\sum_{i}^{\boldsymbol{Desired\ Products}} (\boldsymbol{C_i} * \boldsymbol{N_{Ci}})}{\sum_{i}^{\boldsymbol{All\ Products}} (\boldsymbol{C_i} * \boldsymbol{N_{Ci}})}$$

$$\boldsymbol{Conversion} = \frac{\sum_{i}^{\boldsymbol{All\ Products}} (\boldsymbol{C_i} * \boldsymbol{N_{Ci}})}{\sum_{i}^{\boldsymbol{All\ Products}} (\boldsymbol{C_i} * \boldsymbol{N_{Ci}}) + \boldsymbol{C_{Methane}}}$$

$$\boldsymbol{Yield} = \boldsymbol{Selectivity} * \boldsymbol{Conversion}$$

Figure 12: Definitions for performance benchmarks

3. Results and Discussion

3.1 COC Cycle Behavior and Activation Results

The COC underwent 10 cycles of reduction in CH_4 then oxidation in air to become activated. From preliminary TGA studies, the catalyst lost and regained 4.7% of its weight during each cycle of reduction followed by oxidation which approximately equates approximately to the cycling of $Li_{0.2}Mg_{5.8}MnO_8 \leftrightarrow Li_{0.2}Mg_{5.8}MnO_7$ as shown for TGA results of 1 cycle in Figure 13 below. Although this chemical equation for the solid COC cycling is closely reflected in the weight change seen, advanced experimental methods performed on a non-lithium-doped Mg_6MnO_8 system point to a mixture of metal oxides that result from reduction rather than a single phase [19].

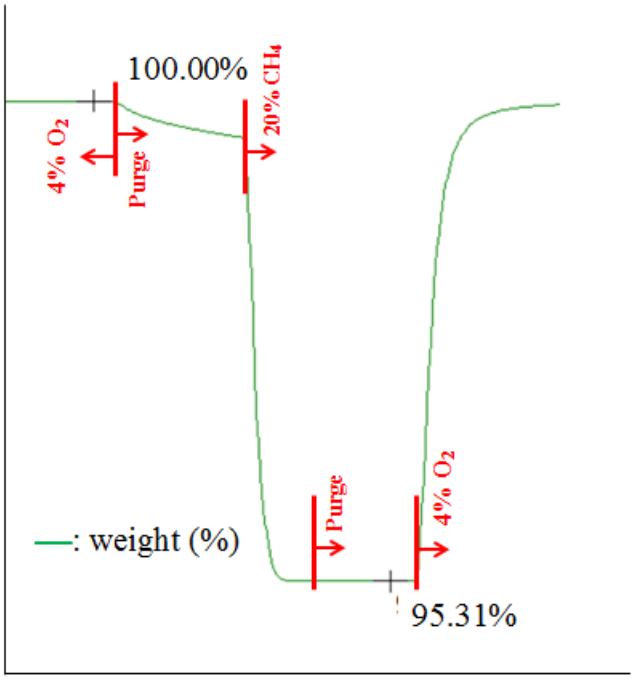

Figure 13: TGA results of weight loss during full reduction

The cycling of the COC to achieve activation was initially deemed necessary by the identification of reactivity changes that occurred during the first few cycles of the COC's

activation. In these studies, pure methane was reacted for 15 seconds with the first 5 seconds of reactivity captured and analyzed to determine the product-make of the COC. It was then reoxidized under the flow of air for 30 minutes. As shown in Figure 14 below, as the number of cycles that the COC was exposed to increased, the COC's conversion of methane increased while its selectivity towards desired C_2+ products decreased. These changes taper off around the 6th and 7th cycles. Therefore, 10 cycles was determined to be adequate for activation of the COC. This required cyclic activation period is common in complex metal oxide systems where the COC's reactivity characteristics become stable after around 10 cycles [20].

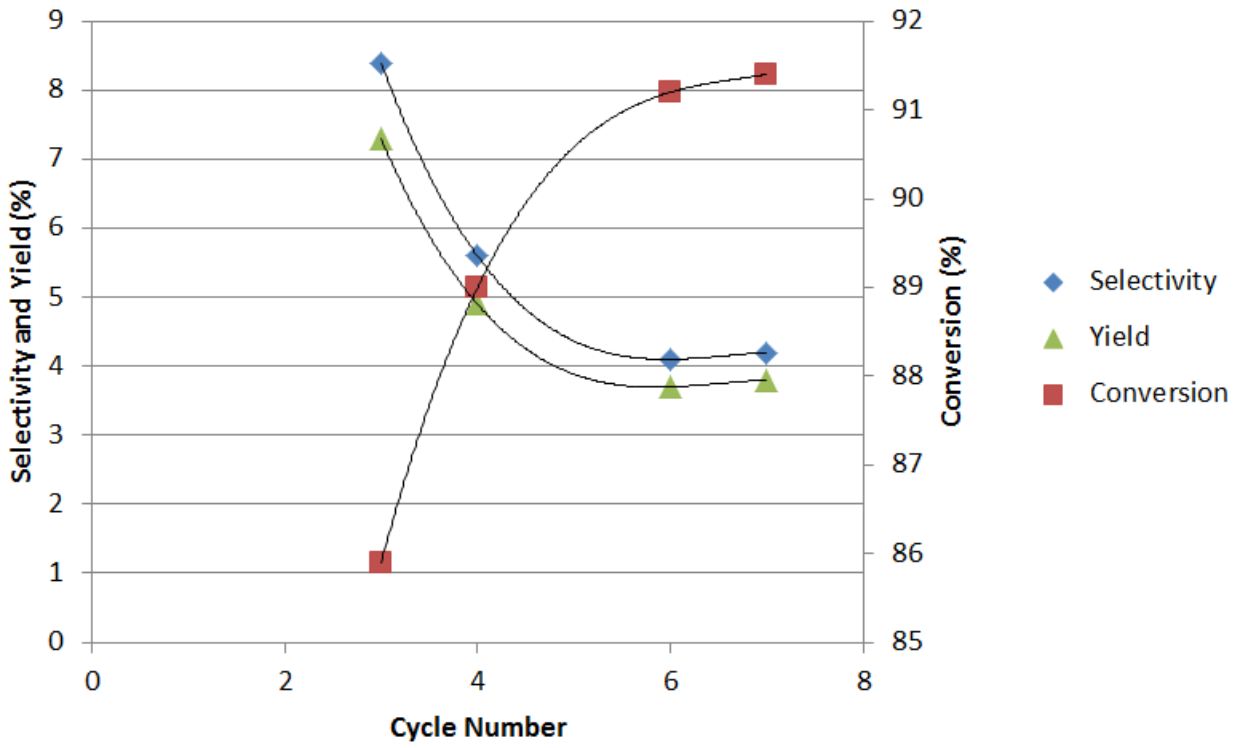

Figure 14: Cyclic fixed bed reactivity results for 0-5 seconds of reactivity indicating the need for COC activation

To confirm these reactivity findings, cyclic TGA studies were performed on fresh COC to evaluate mass changes of the COC during activation. The results for 8 cycles are shown in Figure 15 below. During the cycle, N_2 is used to purge any gaseous oxygen then 20% methane is

introduced. When the methane is introduced, significant weight loss occurs as a result of reduction of the COC. As shown in the figure, the maximum instantaneous rate of weight loss during reduction (shown as the peaks in red) increases steadily with each cycle before leveling off after the 8th cycle. The greater maximum rates of weight loss for the later cycles coincides with the greater conversion and lower selectivity of these later cycles seen in the reactivity studies and confirms the reactivity study findings.

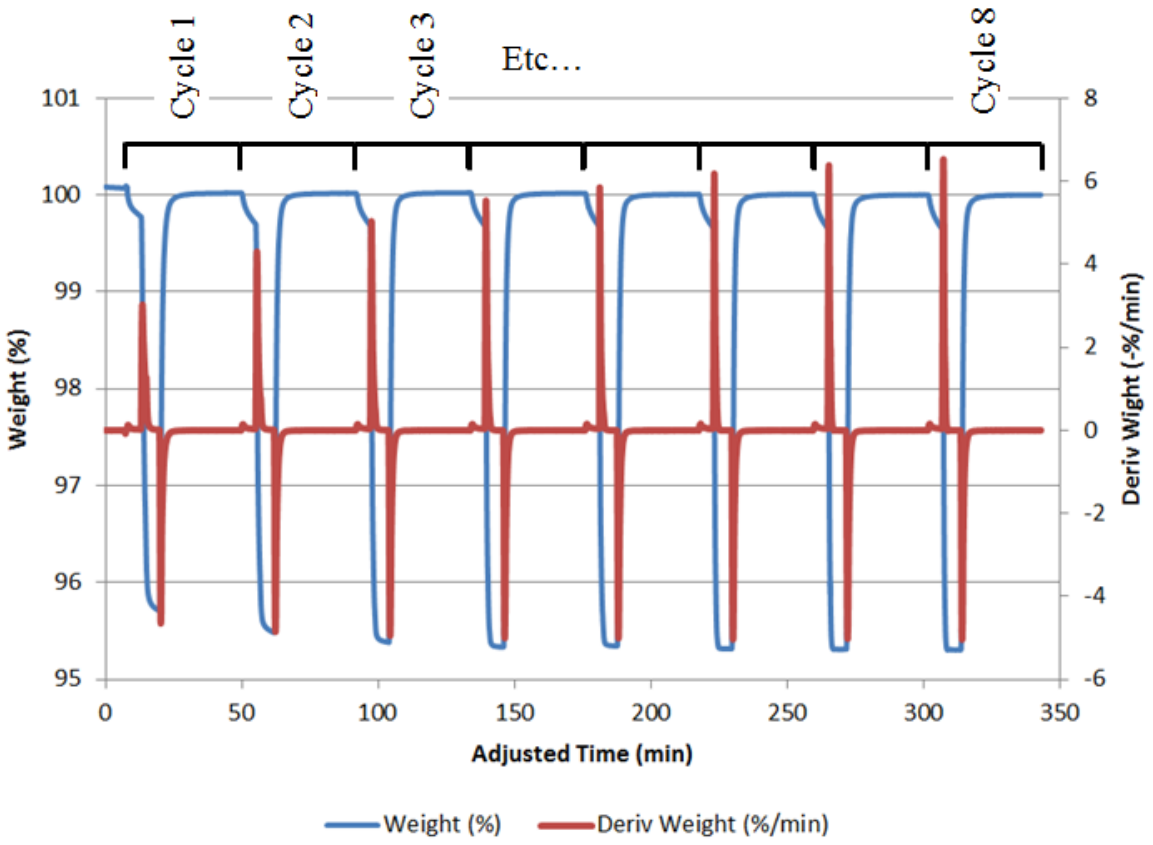

Figure 15: Increase in maximum instantaneous rate of weight loss (red) as cycles increase

In an effort to better understand what changes were occurring during these activation cycles, surface area changes were analyzed using the BET approach [21] and the results are presented in Table 2 below. These changes indicate that some sintering of the COC occurred as oxygen was lost during reduction and then re-captured during oxidation reducing the total surface area. This

decrease in surface area would typically be expected to decrease the activity of the COC and therefore the conversion, however, since conversion actually increased, it is apparent that some other phenomena is causing the increase in conversion that it is not related to the number of active sites. One possible explanation is that the cycling of COC creates lattice oxygen point defects in the bulk lattice. These defects might result from insufficient oxidation time to fill all of the oxygen vacancies formed during reduction. However, as seen in other studies, the oxygen vacancies are few enough to not change the ideal stoichiometry of the COC but are numerous enough to have effects on intra-particle oxygen diffusion [22]. These oxygen defects would increase the bulk oxygen diffusion rate to the surface explaining the increase in maximum rate of oxygen loss during reduction and the increase in conversion [23]. Computational studies of another OCM COC's support this hypothesis by indicating that the rate oxygen diffusion is associated with an interlayer vacancy mechanism in the COC [22]. This theory, however, would need more advanced experimental and computational techniques for testing.

Table 2: Surface area measurements for fresh and 10 cycle activated COC

BET Surface Area (m^2/g)	
Fresh, Oxidized COC	Activated, Oxidized COC
0.955	0.908

3.2 TGA Results

The first TGA study performed focused on changes in the relative weights of the oxidized, N_2 reduced, and fully reduced COC to make estimations as to the oxidation state of manganese. Manganese is necessary for the gain/loss of lattice oxygen as it is the only metal present that can exist at multiple oxidation states. The results of this first TGA study are shown below in Figure 16. As can be seen in the figure, under the steady flow of N_2, the COC

underwent partial reduction resulting in a weight loss of 2.9%. This weight loss is directly related to the loss of uncoupling oxygen. Under full reduction, the COC undergoes a total weight-loss of 4.7% due to loss of the rest of its strongly bound lattice oxygen which accounts for 1.8% of the COC's total weight. Comparing the N_2 reduced COC with the fully reduced COC, the N_2 reduced COC has lost around 60% of its available oxygen. Given that in the fully oxidized COC, the manganese has an approximate oxidation state of 4+, the N_2 reduced COC has a mixture of manganese at oxidation states of 3+ and 2+ while the fully reduced COC has manganese at oxidation state of 2+.

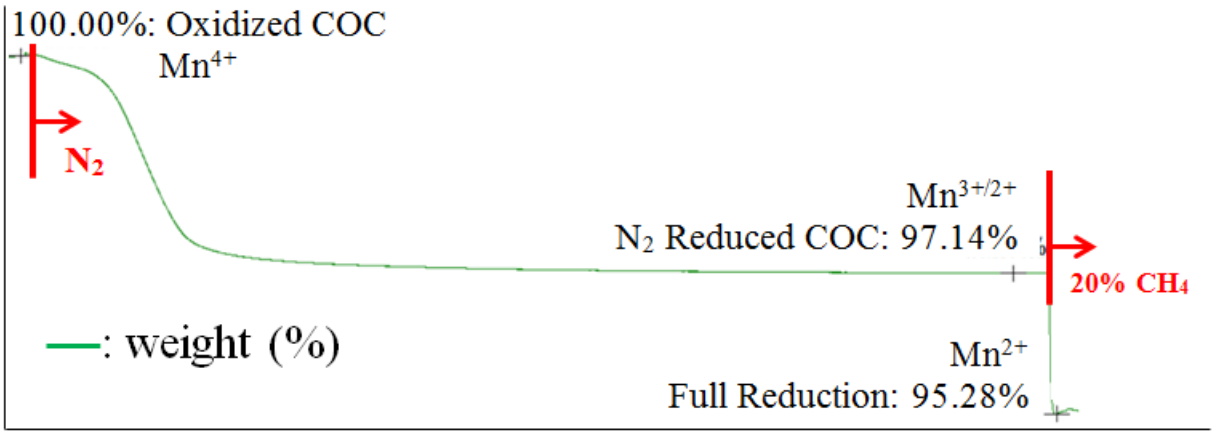

Figure 16: Weight loss resulting from partial reduction in N_2 and full reduction in CH_4

In the second TGA study, the relative rates of reduction of the oxidized and N_2 reduced COC's were compared by pulsing in 20% methane and measuring the maximum instantaneous rate of weight-loss. As shown in Figure 17 below, the oxidized COC's maximum rate of weight loss was 3.25 times faster than that for the N_2 reduced COC (-6.525%/min for oxidized COC compared to -2.043%/min for N_2 reduced COC). This high rate of oxygen delivery to the process is expected to increase conversion while having a negative effect on yield.

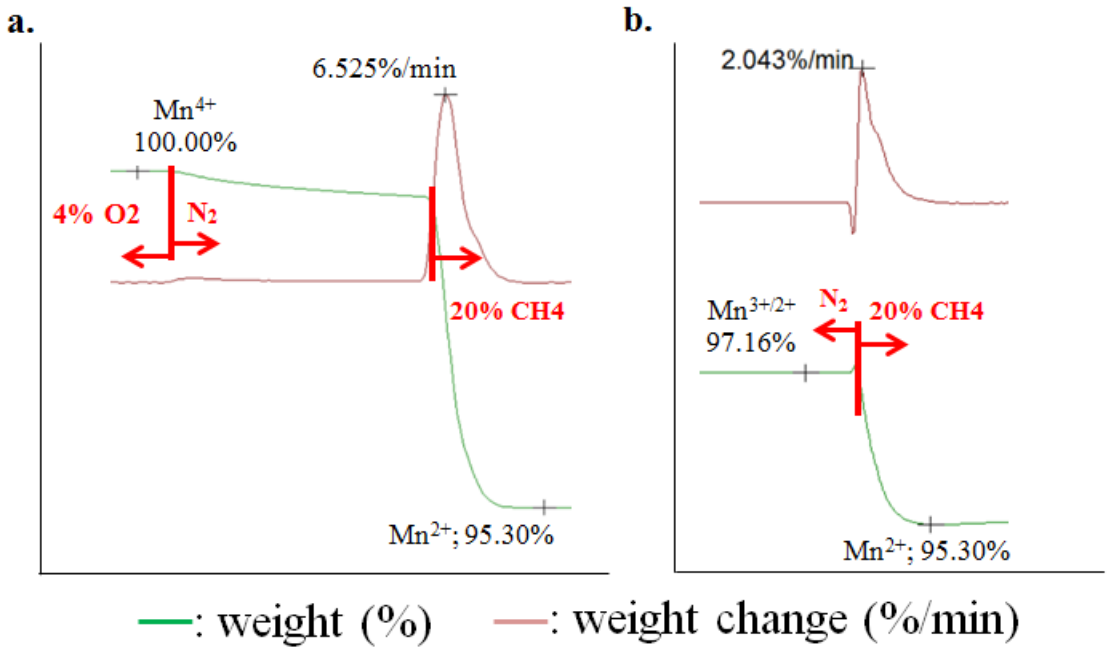

Figure 17: Relative rates of reduction for (a) oxidized COC and (b) N_2 reduced COC

To identify the effects of the oxidation state on the reactivity of the COC, the trends of a previous study from the same lab will be presented and compared [18]. In this study, the oxidized and N_2 reduced COC were exposed to a short pulse of methane and the products for the first 5 seconds of reaction were analyzed. The trends of these results are summarized in Table 3 alongside a summary of the TGA results. As shown in the table, the high rate of instantaneous oxygen delivery by the oxidized COC resulted in over-oxidation of hydrocarbons species and high CO_2 formation shown by the low selectivity. The slowed rate of instantaneous oxygen delivery for the N_2 reduced COC minimized the over-oxidation of hydrocarbon species resulting in higher selectivity but a lower conversion.

Table 3: Summary results of TGA and fixed bed studies

	TGA Results		Initial Fixed Bed Results	
COC	Relative Weight	Instant. Rate of Weight Loss (%/min)	Selectivity (%)	Conversion (%)
Oxidized	100.0%	-6.53	Low	High
N_2 Reduced	97.2%	-2.04	High	Low

From these reactivity and TGA studies, it was hypothesized that the simulated co-current configuration would give better yields than the counter-current configuration. The reasoning behind this hypothesis is that placing the more selective N_2 reduced COC reactor bed second in the reaction flow would prevent over-oxidation of any products formed in the first reactor bed. The simulated counter-current moving bed, on the other hand, would have the less selective, oxidized COC bed second in the reaction order which would over-oxidize most products formed in the first reactor bed since combustion of the primary product, ethene, has been found to occur 3 to 5 time faster than the combustion of methane [24].

3.3 Simulated Moving Bed Results

To test the hypothesis from section 3.2 and determine which moving bed configuration might provide the best yields, the simulated co-current and counter-current moving bed reactors were tested as described in section 2.3. The product distributions of the co-current and counter-current moving bed configuration are shown below in Table 4. In addition, selectivities, conversions and yields of the two reactor configurations for the first 5 seconds of reaction are compared in Figure 18 below.

Table 4: Product distributions for co-current and counter-current simulated moving bed reactor tests

Product Gas Distribution	Co-Current Simulated Moving Bed		Counter-Current Simulated Moving Bed	
Compound	0-5s	5-10s	0-5s	5-10s
Methane	0.427	0.430	0.346	0.474
CO_2	0.533	0.523	0.614	0.497
CO	0.000	0.015	0.000	0.000
Ethane	0.015	0.011	0.013	0.011
Ethylene	0.017	0.013	0.022	0.015
Acetylene	0.001	0.000	0.004	0.001
Propane	0.000	0.000	0.000	0.001
Propylene	0.001	0.000	0.000	0.001
C5's	0.005	0.005	0.000	0.002
Selectivity	15.2%	12.8%	10.7%	12.8%
Conversion	59.6%	59.0%	66.5%	54.6%
Yield	9.1%	7.6%	7.1%	7.0%

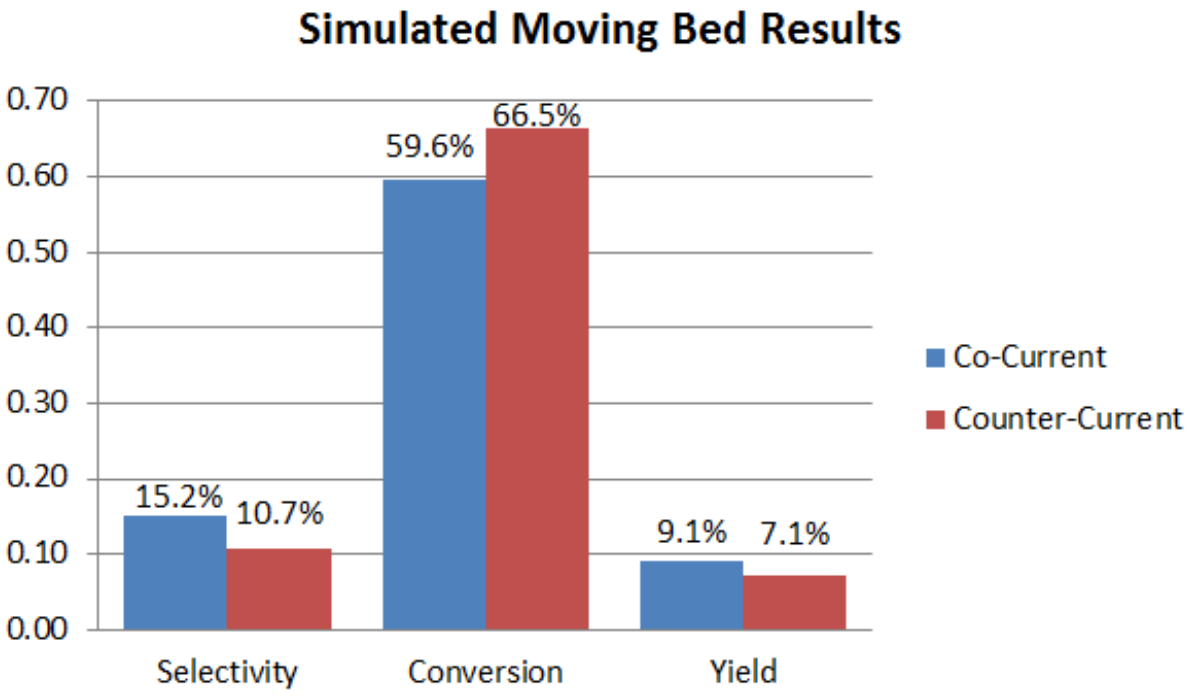

Figure 18: Reactivity summary for the first 5 seconds of reaction for simulated moving bed configurations

As shown in the results for the first 5 seconds of reaction, the simulated co-current moving bed configuration gave a 28% increase in over than the simulated counter-current moving bed configuration. This yield increase was brought about by a large increase in selectivity (>40% increase) while maintaining a similar conversion. This validates the earlier hypothesis that an improvement in yield could be achieved in the simulated co-current configuration due to the minimization of over-oxidation of products by placing the more selective N_2 reduced COC reactor bed second in the reactor order.

4. Conclusion and Future Work

A selectively active catalytic oxygen carrier (COC) for the oxidative coupling of methane (OCM) was synthesized, activated, and its reduction/oxidation properties and reactivity were characterized. Under the flow of pure N_2 at 850°C, the COC partially reduces losing 2.9% of its total weight as a result of its loss of uncoupling lattice oxygen. This is around 60% of its total available oxygen because under pure methane, the COC became fully reduced resulting in a total weight loss of 4.7%. The partial loss of oxygen for the N_2 reduced COC drastically changed its reactivity behavior under the flow of pure methane causing a significant increase in selectivity towards ethene, ethane, and higher hydrocarbon products coupled with a reduction in methane conversion.

These changes in reactivity for the N_2 reduced COC led to the hypothesis that a co-current moving bed reactor would provide better yields for an OCM process using a chemical looping reaction scheme. This is due to the profile of the COC in the moving bed reactor. In a co-current configuration, the reactant gases initially contact a fully oxidized COC with maximum lattice oxygen concentration and the COC's oxidation state steadily decreases as it moves through the reactor. This decrease in oxidation state results in a significant reduction of available lattice oxygen of the COC at the outlet of the reactor and minimizes the possibility of over-oxidation in the latter part of the reactor of any products that were formed in the initial sections of the reactor resulting in improved yields. This is in contrast to the counter-current moving bed configuration where the oxidized COC enters the reactor at the opposite side of the gas outlet. In this configuration, any products formed in the early sections of the reactor must contact a fully oxidized COC with maximum available lattice oxygen before exiting the reactor. This increases

the chances of over-oxidation of any products that may be present which is detrimental to the product yield.

To test this hypothesis, a moving bed reactor was experimentally simulated using two fixed bed reactors. The co-current moving bed configuration was simulated by placing fully oxidized COC in the first reactor bed and N_2 reduced COC in the second reactor bed reflecting roughly the COC profile that would be found in a true co-current moving bed reactor. The counter-current moving bed configuration was simulated in the opposite manner placing the N_2 reduced COC in the first bed and the oxidized COC in the second bed reflecting the profile of a counter-current moving bed reactor.

The results from these experiments showed that for the co-current simulated moving bed reactor, selectivities increased around 40% over the counter-current simulated moving bed reactor while the conversions were similar. This resulted in a yield of 9.1% for the simulated co-current configuration and only a 7.1% yield for the simulated counter-current configuration and validated the hypothesis that a co-current moving bed reactor could provide increased yield and provides a direction forward for scale-up to a bench-scale true moving bed reactor.

Further experiments could include operation of a bench-scale moving bed reactor to determine if the predictions made from the results of the two-fixed-bed reactor hold true. This would validate the simplifying assumptions that two fixed bed reactors could be used to simulate a true moving bed reactor.

References

1. The Ethylene Technology Report 2016. *Research and Markets*. February 2016. Available at: http://www.researchandmarkets.com/research/2xl4dr/the_ethylene.
2. U.S. Energy Information Administration. Total Energy Visualization. *EIA Web site*. 2017. Available at: https://www.eia.gov/totalenergy/data/browser/?tbl=T04.01#/?f=A&start=2006&end=2016&charted=3-8-11. Accessed April 1, 2017.
3. Keller GE, Bhasin MM. Synthesis of Ethylene via Oxidative Coupling of Methane. *J. Catal.* 1982;73:9-19.
4. Zavyalova U, Holena M, Schlogl R, Baerns M. Statistical Analysis of Past Catalytic Data on Oxidative Methane Coupling for New Insights into the Composition of High-Performance Catalysts. *Chem. Cat. Chem*. 2011;3:1935-1947.
5. Mars P, van Krevelen DW. Oxidations Carried Out by Means of Vanadium Oxide Catalysts. *Special Supplement to Chemical Engineering Science*. 1954;3:41-59.
6. Alkhatib H. Analysis of Varied Feedstocks for Oxidative Coupling of Methane Catalyst in a Redox Configuration. *Undergraduate Thesis. Retrieved from OhioLINK*. 2016.
7. Zimmermann H, Walzl R. "Ethylene". In: Elvers B, ed. *Ullmann's Encyclopedia of Industrial Chemistry*. Weinheim: Wiley; 2014.
8. Su YS, Ying JY, Green WH. Upper Bound on the Yield for Oxidative Coupling of Methane. *J. Catal.* 2003;218:321-333.
9. Labinger JA. Oxidative Coupling of Methane: An Inherent Limit to Selectivity? *Catal. Lett.* 1988;1:371-376.

10. Corma A, Martinez A. "Transformation of Alkanes on Solid Acid and Bifunctional Catalysts". In: Derouane E, Haber J, Lemos F, Ribeiro F, Guisnet M, eds. *Catalytic Activation and Functionalization of Light Alkanes: Advances and Challenges*. Vilamoura: Springer; 1997.

11. Chung EY, Wang WK, Nadgouda SG, Baser DS, Sofranko JA, Fan L. Catalytic Oxygen Carriers and Process Systems for Oxidative Coupling of Methane Using the Chemical Looping Technology. *Ind. Eng. Chem. Res.* 2016;55:12750-12764.

12. Sofranko JA, Leonard JJ, Jones CA. The Oxidative Conversion of Methane to Higher Hydrocarbons. *J. Catal.* 1987;103:302-310.

13. Wolff EHP, Veenstra P, Chewter LA. A Novel Circulating Cross-Flow Moving Bed Reactor System for Gas-Solids Contacting. *Chem. Eng. Sci.* 1994;49:5427-5438.

14. Luo S, Zeng L, Xu D, et al. Shale Gas-to-Syngas Chemical Looping Process for Stable Shale Gas Conversion to High Purity Syngas with a H2:CO Ratio of 2:1. *Energy Environ. Sci.* 2014;7:4104-4117.

15. Larkins FP, Nordin MR. The Effects of Transition Metal Oxides on the Methane Oxidative Coupling Activity of Doped MgO Catalysts I. Zinc and Manganese. *J. Catal*. 1991;130:147-160.

16. Larkins FP, Nordin MR. Oxidative Dehydrogenation of Methane to Form Higher Hydrocarbons. In: Bibby DB, Chang CD, Howe RF, Yurchak S, eds. *"Methane Conversion"*. Vol 36. Amsterdam: Elsevier; 1988.

17. Korf SJ, Roos JA, Veltman LJ, Van Ommen JG, Ross JRH. Effect of Additives on Lithium Doped Magnesium Oxide Catalysts Used in the Oxidative Coupling of Methane. *Appl. Catal.*

1989;56:119-135.

18. Jindra M. Unpublished Manuscript: Undergraduate Thesis. *Unpublished*. 2017.

19. Golikov YV, Barkhatov VP, Balakirev VF, Chufarov GI. Thermal Dissociation of Mg6MnO8. *Russian Journal of Inorganic Chemistry*. 1982;27:934-936.

20. Sung JS, Choo KY, Kim TH, et al. Peculiarities of Oxidative Coupling of Methane in Redox Cyclic Mode Over Ag-La2O3/SiO2 Catalysts. *Appl. Catal. A*. 2010;380:28-32.

21. Brunauer S, Emmett PH, Teller E. Adsorption of Gases in Multimolecular Layers. *J. Amer. Chem. Soc.* 1938;60:309-319.

22. Ilett DJ, Islam MS. Role of Structural Defects and Oxygen Ion Migration in the Catalytic Activity of La2O3. *J. Chem. Soc. Faraday Trans.* 1993;89:3833-3839.

23. Martin M. Diffusion in Oxides. In: Heitjans P, Karger J, eds. *Diffusion in Condensed Matter: Methods, Materials, Models*. Berlin: Springer; 2005.

24. Shi C, Rosynek MP, Lunsford JH. Origin of Carbon Oxides durng the Oxidative Coupling of Methane. *J. Phys. Chem.* 1994;98:8371-8376.